rspa.royalsocietypublishing.org

Research

Article submitted to journal

Subject Areas:
pattern formation, synchronisation, nonlinear dynamics, cold-atom optics

Keywords:
optomechanics, self-organisation, Kuramoto model, long range interactions, cold atoms

Author for correspondence:
Corresponding Author
e-mail: g.r.m.robb@strath.ac.uk

Self-organisation in cold atomic gases: a synchronisation perspective

E. Tesio[1], G. R. M. Robb[1], G.-L. Oppo[1], P. M. Gomes[1], T. Ackemann[1], G. Labeyrie[2], R. Kaiser[2], W. J. Firth[1]

[1]SUPA and Department of Physics, University of Strathclyde, 107 Rottenrow East, Glasgow G04NG, UK
[2] Institut Non Linéaire de Nice, UMR 7335 CNRS, 1361 route des Lucioles, 06560 Valbonne, France

We study non-equilibrium spatial self-organisation in cold atomic gases, where long-range spatial order spontaneously emerges from fluctuations in the plane transverse to the propagation axis of a single optical beam. The self-organisation process can be interpreted as a synchronisation transition in a fully connected network of fictitious oscillators, and described in terms of the Kuramoto model.

1. Introduction

In recent years, cold and ultracold matter have proved to be a formidable tool for the investigation of phase transitions and collective behaviour in non-equilibrium systems. When coupling the dynamics of light and the center-of-mass degrees of freedom of laser-cooled atoms, the dynamics becomes nonlinear and, above a critical value for the energy injected into the system, a transition is observed from a spatially homogeneous state to a state displaying some form of long-range order. This can be obtained in various configurations: transversally pumped cavities [1] where collective dynamics and self-organisation in cold [2,3] and ultracold [4] gases have been investigated; collective atomic recoil lasing (CARL) where the spontaneous generation of a back-scattered beam within a monodirectional cavity is self-sustained by atomic bunching in the resulting optical potential [5–7]; in a counter-propagating geometry superradiance and high-order nonlinearities stemming from atomic bunching have been studied [8–10]. The spontaneous breaking of a continuous translational symmetry in the presence of a strong viscous damping was investigated both for cavity [11,12] and counter-propagating [10,13,14]

geometries, while a single-mirror geometry in the absence of damping was the focus of recent theoretical [15] and experimental [16] research. The distinguishing feature of these studies is that the spatial scale of the emerging spatial structure is self-selected, so that the spontaneous breaking of two continuous symmetries is observed (rotations and translations in the plane). A fully connected network is implemented through effective long range interactions mediated by the optical fields, so that a mean-field model effectively captures the dynamics of the system [11,15]. The same general concept lies at the heart of much recent research, ranging from the atom-optical simulation of condensed matter phenomena [1] to the the study of spin-glass transitions in cold atoms [17].

Together with spatial self-ordering, another prominent feature of nonlinear systems is that of temporal spontaneous ordering, i.e. synchronisation. The emergence of synchronisation is a pervasive feature of nonlinear science, ranging from biology and chemistry to neuroscience and social networks [18]. Broadly speaking, the spatial ordering into a periodic structure and the synchronisation of oscillators on a limit cycle can be thought of as the same phenomenon, if the extended nature of the spatial coordinate is ignored, and only the spatial phase is considered. Implementing light-mediated atom-atom interactions opens the possibility for tunable and controllable realisations of long-range interacting and mean-field models for synchronisation [19], and indeed this was exploited in Refs. [7,20] to connect the viscous CARL dynamics to the Kuramoto model for synchronisation of coupled oscillators [21]. We will show in the following that this connection is not limited to CARL, but applies also to the symmetry-breaking transverse instabilities studied in [15,16]. Moreover, the connection made in [7,20] referred to the case where strong damping is present in the system (hence the denomination 'viscous' CARL), which in the Kuramoto analogy translates into the case where the oscillators have zero natural frequencies (their distribution is a Dirac delta function). We extend here the Kuramoto analogy to the situation analysed in [15,16], where no damping is present and a finite spread exists in the natural frequency distribution of the fictitious oscillators.

2. Single-mirror optomechanical instabilities

(a) Basic scheme

We consider the single-mirror setup [22] depicted in Fig. 1, where a cold gas of two-level atoms is illuminated from the side by a pump beam of amplitude F, frequency ω_0 and wavenumber k_0. The pump beam is detuned by $\delta = \omega_0 - \omega_{\rm at}$ from the atomic transition (frequency $\omega_{\rm at}$, linewidth Γ), and is retroreflected by a mirror of reflectivity R placed at distance d from the cloud to form the backward beam (amplitude B). We can thus envisage a situation where fluctuations in the atomic spatial properties can modify the refractive index distribution in the atomic ensemble and in turn the phase profile of the field. These phase fluctuations are converted into amplitude fluctuations by the free-space propagation to the mirror and back (related to the Talbot effect [23]) [24,25]. If the medium is nonlinear, it will react to these amplitude perturbations resulting in a runaway, self-organisation process where initial fluctuations are exponentially amplified and a macroscopic structure, emerging from noise, is encoded in the spatial properties of the atomic cloud. These spatial perturbations can be in the internal states of the atoms, e.g. a change of population of the excited state (electronic or two-level nonlinearity) or Zeeman sublevel (optical pumping nonlinearity) or in the external degrees of freedom of the atoms. In particular we are interested here in the centre of mass, motional degrees of freedom of the atoms, which can be excited by dipole forces. As was first established for dielectric beads [26–28], linear Rayleigh scatterers can exhibit a significant optomechanical nonlinearity: for a negative polarisability (corresponding to $\delta > 0$ for atoms), the dielectric scatterers are low-field seekers and are expelled from high intensity regions. Since for $\delta > 0$ the refractive index of atoms is smaller than one, a decrease in atomic density implies an increase of refractive index. Hence the refractive index increases where

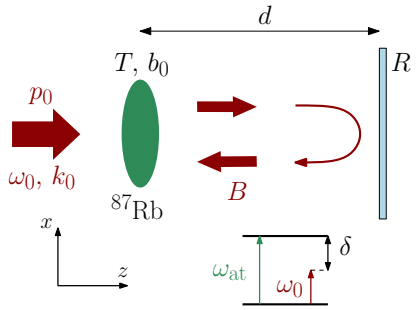

Figure 1: Sketch of the single-mirror setup. A pump beam with an intensity corresponding to a saturation parameter $p_0 = |F|^2$, frequency ω_0 and wavenumber k_0 illuminates a dense cloud of cold ^{87}Rb (temperature T, optical density in line centre b_0). The beam is phase-shifted and transmitted from the cloud, and then retroreflected as the backward (B) beam after propagation to the mirror (distance d, reflectivity R) and back.

the intensity is high, leading to an effective self-focusing nonlinearity. The result is a *transverse optomechanical instability*.

(b) Basic experimental observations

In the experiments motivating our study [16] the D_2 line of ^{87}Rb is exploited (transition wavelength $\lambda_0 = 780.27\,\mathrm{nm}$) with an excited state lifetime of $\Gamma^{-1} = 26\,\mathrm{ns}$. An atomic ensemble is laser-cooled in a magneto-optical trap (MOT) to a temperature of about 290 μK. At this temperature Doppler broadening is negligible compared to the linewidth of the atomic transition ($\Gamma/(2\pi) = 6.06$ MHz). The cold sample obtained has a roughly Gaussian density profile with dimensions (full-width-at-half-maximum, FWHM) of $10 \times 10 \times 5$ mm (10 mm along the propagation direction) and contains about 5×10^{10} atoms. The optical density in line centre is $b_0 = 150$. Then the MOT (trapping lasers and magnetic field) is shut down and the pump beam is turned on for a duration t_{pump}. This pump beam is spatially filtered by a single-mode fibre and collimated to a spot size of 1.9 mm (FWHM). The experiment is performed in the vicinity of the $F = 2 \to F' = 3$ hyperfine transition, which is closed. A repumper tuned to the $F = 1 \to F' = 2$ transition counteracts hyperfine pumping due to the residual excitation of other states. The polarisation of the pump beam is linear. Details of the setup can be found in [16].

Spontaneous breaking of transverse symmetries and pattern formation are observed for a wide range of positive detunings to the $F = 2 \to F' = 3$ transition, most experiments being done with a pump detuning in the range $\delta = 7 - 10\,\Gamma$. The observed patterns have hexagonal symmetry and consist of well developed peaks. As we are going to compare the results to a one-dimensional theory, we are presenting here only cross-sections of the two-dimensional structures. The upper panel of Fig. 2 shows a section through the light pattern in the pump beam. A high modulation is evident with peaks reaching 3.5 times the background of the input beam. The pattern wavelength is about 110 μm and is found to depend on the feedback distance [16].

Ten microseconds after the pump beam is switched off, a weak probe beam, which is orthogonally polarised to the pump and does not experience feedback, is injected into the medium. It is detuned a few linewidths to the low-frequency side of the resonance and shows a honeycomb pattern. For the dispersive imaging situation used here, one expects that high intensity levels are obtained where the refractive index in the sample is high. For negative detunings these are the regions with a high atomic density. The observation of honeycombs is hence consistent with the expectation for complementary patterns in the light field and the atomic density: atoms are expelled from the pump filament and gather along the ridges of the honeycomb pattern.

Within ten microseconds, all excited state populations created by the pump will have decayed.

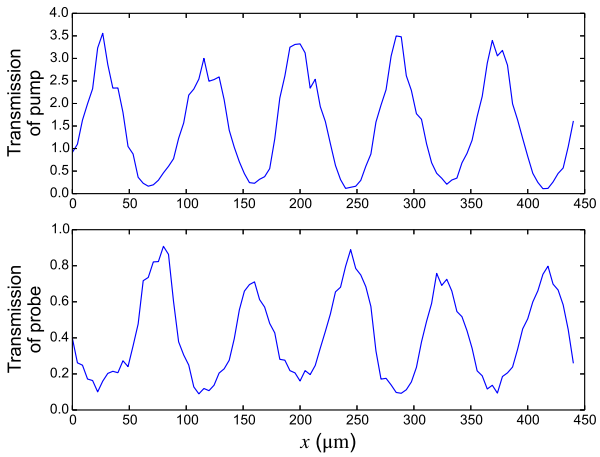

Figure 2: Cross-sections of typical hexagonal patterns observed in the transmitted pump beam (upper panel) and probe beam (lower panel). Both stem from the re-imaged intensity distribution 10 mm after the cloud (i.e. corresponding to the reentrant backward beam) and are normalized to the input intensity without atoms. Parameters for the pump beam: $I = 129\,\mathrm{mW/cm^2}$, $\delta = +7\ \Gamma$, and $d = 5$ mm; for the probe beam $\delta = -7\ \Gamma$.

Hence the presence of a structure a few microseconds after the pump beam is switched off excludes electronic excitation as the source of the atomic grating evidenced by the probe. As other measurements exclude hyperfine and Zeeman gratings [16], we conclude on the presence of a significant density grating in the atomic cloud. This can be further substantiated by investigating the dependence of the contrast of the probe pattern on the delay time between pump and probe pulse. The result is shown in Fig. 3, which gives a decay time of around 80 μs (corresponding to a decrease of the contrast by a factor of two). As an atom with a 1D thermal speed of $0.17\,\mathrm{m/s}$ would traverse $55\,\mu$m (half the transverse period) in about $300\,\mu$s, this is a reasonable order of magnitude for a wash-out of a density pattern due to the velocity spread of the ensemble. This will be explored further in the theoretical section.

3. Theoretical model

The analysis of the experimental results is somewhat complicated by the fact that in general electronic and optomechanical nonlinearities are simultaneously present, so that an internal-state and a density pattern can be simultaneously present in the atomic ensemble. Internal-state nonlinear effects can be accounted for in our theoretical model [16] but we will neglect them here by assuming low saturation values, since at low temperatures a spatial instability is expected to occur even at low saturation levels due to density redistribution effects only [15]. The results presented in [16] provide experimental support for this claim in the appropriate parameter regimes.

For a theoretical treatment, we consider in the following the case of a cigar-shaped cloud elongated along the coordinate x transverse to the propagation direction z, so that transverse self-organisation will lead to one-dimensional structures. Our theoretical analysis [15] indicates in fact that no qualitative differences are expected for the dynamics of one and two-dimensional systems, and restricting to one dimension allows for a connection with temporal synchronisation phenomena. We neglect propagation inside the cloud and account for diffraction of the transmitted field only in the free-space propagation to the mirror and back. For the parameters

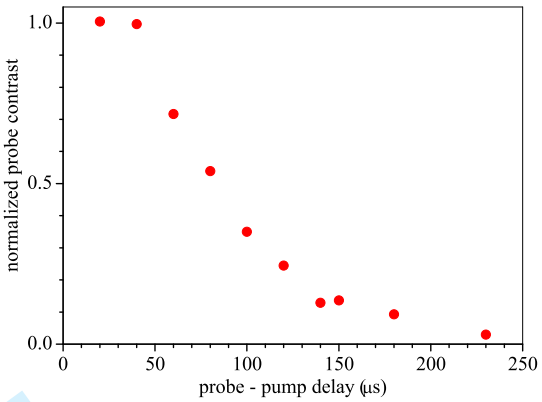

Figure 3: Decay of the density pattern (as measured by the probe) as the delay between pump (duration 215 μs) and probe (duration 10 μs) pulses is increased. Other parameters are pump detuning $+7\Gamma$, probe detuning $+5\Gamma$, pump power 6.6 mW, probe power 20 μW. Pump and probe are circularly polarised. The contrast is normalised to the contrast just after the pump switch-off.

considered here, this simplifying assumption provides good qualitative agreement with more detailed models in which diffraction within the medium is also taken into consideration, as discussed in [16]. We also assume the pump to be substantially detuned from the atomic resonance, so that that the atoms act as linear scatterers and the transmitted field $F_{\rm tr}$ at the exit of the cloud is:

$$F_{\rm tr}(x,t) = F\exp\left(i\chi_0 n(x,t)\right) \tag{3.1}$$

where $\chi_0 = b_0\Delta/(1+4\Delta^2)$ parametrizes the cloud susceptibility and $\Delta = \delta/\Gamma$. Scaling of the field is chosen so that $p_0 \equiv |F|^2 = \frac{I_{\rm pump}}{I_{\rm sat}(1+4\Delta^2)}$ denotes the off-resonance saturation parameter of the pump, where $I_{\rm pump}$ is the pump intensity and $I_{\rm sat}$ is the on-resonance saturation intensity ($I_{\rm sat} = 1.6 - 3.6{\rm mWcm}^{-2}$ for the D_2 line of ^{87}Rb, depending on the exact excitation conditions). In the limit of large number of atoms N ($N \sim 10^{10}$ in a typical experiment) we describe the cloud dynamics in terms of a phase-space distribution $f(x,v,t)$, where v is the transverse velocity coordinate, so that the atomic density is obtained as

$$n(x,t) = \int_{-\infty}^{+\infty} dv\, f(x,v,t)\,.$$

As the gas is cooled to relatively low temperatures, $T \sim 100\,\mu$K, optical forces become relevant for the centre-of-mass dynamics of the gas. In particular, at large detuning radiation pressure is reduced and the atoms are subject to the conservative dipole potential $U_{\rm dip} = \frac{1}{2}\hbar\delta\log(1+s(\mathbf{x},t)) \simeq \frac{1}{2}\hbar\delta s(\mathbf{x},t)$, where the last approximation has been taken by assuming the saturation parameter associated with the total intensity illuminating the gas to be small, $s = |F|^2 + |B|^2 = \frac{(1+R)I_{\rm pump}}{I_{\rm sat}(1+4\Delta^2)} \ll 1$. At the low temperatures under consideration collisions are negligible and the dynamics of the gas is captured by the Vlasov equation:

$$\frac{\partial f}{\partial t} + v\frac{\partial f}{\partial x} + \frac{\mathrm{f}_{\rm dip}}{M}\cdot\frac{\partial f}{\partial v} = 0\,, \tag{3.2}$$

where $\mathrm{f}_{\rm dip} = -\partial U_{\rm dip}/\partial x$ is the dipole force and M is the atomic mass. The feedback loop is then closed via diffraction in vacuum described in Fourier space by

$$B(q) = \sqrt{R}\,e^{idq^2/k_0}F_{\rm tr}(q)\,. \tag{3.3}$$

The phasor in Eq. (3.3) describes the conversion of phase fluctuations (imprinted on the transmitted fields via Eq. (3.1)) into amplitude fluctuations by the free-space propagation to the mirror and back. These amplitude modulations in the optical profile result in dipole forces which

consequently act on the atoms and drive the instability.

The coupled light-atom dynamics described above (without internal-state dynamics) is predicted to lead to a self-organising transition when the injected power exceeds a critical value, $p_0 \geq p_0^{\rm th} = (2R\sigma\chi_0)^{-1}$, where $\sigma = \hbar\delta/2k_BT$ measures the strength of dipole forces relative to thermal effects [15]. The spatial scale $\Lambda_{\rm c} = 2\pi/q_{\rm c}$ is set by the critical (most unstable) wavenumber $q_{\rm c} = \sqrt{\pi k_0/2d}$, and can be continuously tuned through the mirror distance d. As $q_{\rm c}$ is selected among a continuum of wavenumbers, the self-structuring mechanism discussed here leads to the spontaneous breaking of a continuous translational symmetry (see Figs. 4c and 4d). Moreover, in two dimensions the rotational symmetry is also broken [16]. This aspect fundamentally differentiates the optomechanical self-structuring investigated here from other self-organising systems involving optomechanics and cold atoms, such as CARL [6,7] and transversely pumped cavities [1–4], as the spatial scale of the emerging structures is not predetermined by the geometrical setup or interference conditions.

4. Synchronisation dynamics and connection with the Kuramoto model

We now discuss the connection between the optomechanical spatial instabilities discussed above and the Kuramoto model for synchronisation. As a starting point, we remark that the spontaneous emergence of a periodic pattern (identified by a single spatial frequency $q_{\rm c}$) can always be interpreted in terms of a synchronisation transition. Focusing on the phase $\theta = q_{\rm c}x$ instead of the spatial coordinate x itself, the bunching of the atoms in the minima of the self-organising optical potential corresponds to the transition from a homogeneous state where the atoms have a uniformly distributed phase to a state where the distribution of the phases is peaked around a certain value ψ. It is convenient in the following to exploit the periodicity of the pattern and confine the phase in the range $(-\pi, \pi)$ as $\theta_j = \mathrm{mod}(q_{\rm c}x_j, 2\pi) - \pi$. This connection between spatial and temporal self-organisation was exploited, for instance, in showing that the spatial instability of viscous CARL can be interpreted in terms of the Kuramoto model [7,20]. Similar results also hold for 'viscous' single-mirror instabilities (see [11,12] for a cavity analogue), but we wish to focus our attention here on the inviscid regime in connection with the experimental results presented in [16].

In order to describe the dynamics of the N atoms composing the gas we consider the $2N$ coupled equations ($j = 1, \ldots, N$)

$$\dot{x}_j = v_j \qquad \dot{v}_j = \frac{\mathrm{f}_{\rm dip}(x_j)}{M} = -\frac{\hbar\delta}{2M}\frac{\partial|B|^2}{\partial x}\bigg|_{x_j},$$

where the force is given by the dipole force $\mathrm{f}_{\rm dip} = -\partial U_{\rm dip}/\partial x$ as above. Since the pump intensity is assumed to be spatially homogeneous, the optical gradients are due only to the backward field modulations. We now obtain an approximate expression for the backward field valid when the system is driven just above the threshold for self-organisation. Close to the critical point, a spatial modulation for the atomic density is obtained at the critical wavenumber, $n(x) = 1 + r\cos(\psi - q_{\rm c}x)$. As the system is translationally invariant, the phase ψ of the pattern is self-selected by the system (see also [20]). The amplitude r and the phase ψ of the pattern define the Fourier mode of the density at the critical wavenumber:

$$re^{i\psi} = \frac{1}{L}\int_0^L n(x)\exp\left(iq_{\rm c}x\right)dx\,, \tag{4.1}$$

so that r acts as an order parameter for the instability. In line with the CARL literature, we refer to r as the *bunching factor*. We stress that while the density spectral properties are directly accessible in numerical simulations, this is not the case in the experimental realisations. A definition analogous to the bunching factor, but based on the Fourier properties of the optical fields, was

termed *contrast* in Ref. [16] and used to experimentally monitor the self-organising dynamics. The same procedure was also used in Fig. 3. In the following we will typically assume that the system is close to the critical point, so that $0 < r \ll 1$. The critical wavenumber is selected by the system as the one that most efficiently converts phase modulations in the pump beam into amplitude modulations for the backward beam [22]. This implies that the far-field sideband at the critical wavenumber is shifted by a factor $e^{i\pi/2} = i$ in the propagation to the mirror and back, so that B is obtained from the transmitted field as (see Eq. (3.3)):

$$F_{\rm tr} \simeq \sqrt{p_0} e^{i\chi_0} \left\{1 + i\chi_0 r \cos(\psi - q_{\rm c} x)\right\} \Longrightarrow B = \sqrt{R p_0} e^{i\chi_0} \left\{1 - \chi_0 r \cos(\psi - q_{\rm c} x)\right\} .$$

To first order in r, the dipole force is thus found as

$$\frac{\mathrm{f}_{\rm dip}}{M} = -\frac{\hbar\delta}{2M}\frac{\partial |B|^2}{\partial x} \simeq \frac{\hbar\delta}{M} R p_0 \chi_0 q_{\rm c} r \sin(\psi - q_{\rm c} x) \equiv J q_{\rm c} r \sin(q_{\rm c} x - \psi) , \tag{4.2}$$

where in the last step we defined $J = \frac{\hbar\delta}{M} R p_0 \chi_0$.

In order to obtain a connection with models for temporal synchronisation, we now wish to use Eq. (4.2) to obtain a single set of N equations for the phases $\theta_j = q_{\rm c} x_j$. Close to the critical point, the modulation depth of the optical potential is small ($r \ll 1$) and the dynamical behaviour of the atoms is force-free in first approximation. This is correct up to a certain time t^*, which we term as *dephasing time*, and has the following interpretation: close to the critical point, the atoms can move freely in the emerging optical potential without affecting the dynamics. This is strictly correct only in the limit of vanishing modulations, $r \to 0$ (i.e. below threshold), but we exploit critical slowing down at the onset of the instability to assume that no feedback on the optical field is exerted by the atomic motion for a characteristic time defined by $t^* = (q_{\rm c} v_{\rm th})^{-1}$. This definition is chosen as the time an atom at the thermal speed needs to travel the characteristic distance of the pattern, $\Lambda_{\rm c} \sim q_c^{-1}$. The equation for the frequencies $\Omega_j = q_{\rm c} v_j$ is then solved up to t^* as

$$\Omega_j(t^*) \simeq \Omega_j(0) + J q_{\rm c}^2 r \sin(\theta_j - \psi) t^* ,$$

where $\Omega_j(0)$ denotes the 'natural' frequencies $\Omega_j(0) = q_{\rm c} v_j(0)$ determined by the initial atomic velocities. The phases then evolve as

$$\dot{\theta}_j = \Omega_j(0) + \frac{J}{v_{\rm th}} q_{\rm c} r \sin(\theta_j - \psi) . \tag{4.3}$$

Eq. (4.3) is in the form of a Kuramoto equation [21], with a coupling strength $K = J q_{\rm c}/v_{\rm th}$. We remark that in Eq. (4.3) an effective long-range interaction between the 'oscillators' (i.e. the atoms) is mediated by the light field, which thus offers the possibility of implementing a mean-field model with all-to-all coupling in a simple and powerful way.

With a Lorentzian initial condition for the natural frequencies $\Omega_j(0)$, the Kuramoto model (4.3) is known to lead to a synchronisation transition when the driving exceeds the critical value $K \geq K^{\rm th} = 2\Omega_{\rm th} = 2 q_{\rm c} v_{\rm th}$ [21]. Hence we recover the power threshold obtained in [15] and reported above: $p_0^{\rm th} = (2R\sigma\chi_0)^{-1}$. As discussed in [15], with a Gaussian initial condition a slightly different growth rate is found for the instability, but the threshold condition is unchanged. Since the synchronisation transition leads to a bunching of the fictitious oscillators around the (self-selected) phase ψ, in the x-space this corresponds to the formation of complementary periodic structures $\sim \cos(q_{\rm c} x - \psi)$ for the atomic density and the optical intensity. We remark that the sign of the optical potential is positive for blue detuning ($\delta > 0$) and negative for red detuning ($\delta < 0$), so that when $\delta > 0$ the density and optical profiles are shifted by half a wavelength (see Figs. 2 and 4). The onset of the optomechanical instability can thus be reinterpreted as a Kuramoto transition to a synchronised state with a self-selected phase ψ where the threshold for this process is determined by the initial spread of the oscillator frequencies. Physically, this spread is determined by the initial temperature of the gas and is therefore tunable experimentally, while the coupling strength K is tunable through the injected pump p_0.

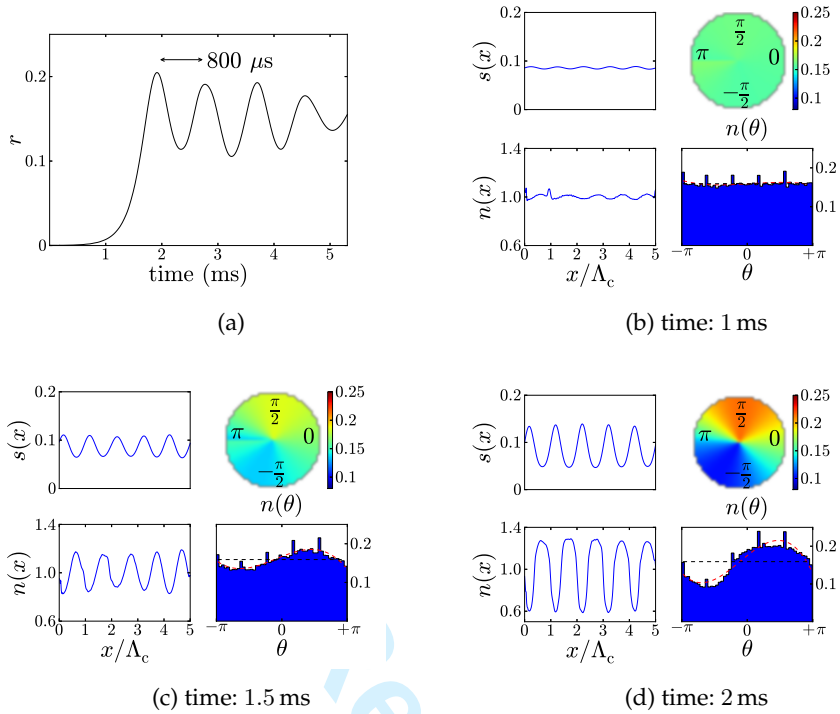

(a) (b) time: 1 ms (c) time: 1.5 ms (d) time: 2 ms

Figure 4: Numerical simulations of the synchronisation dynamics. Fig. a shows the evolution of the bunching factor r, displaying the spontaneous emergence of a macroscopically ordered state after ~ 1 ms followed by oscillations of the order parameter. Figs. b, c and d show snapshots of the dynamics taken after 1 ms (b), 1.5 ms (c) and 2 ms (d). In each of these panels we show the intensity profile $s(x)$ (top left), the density profile $n(x)$ (bottom left), and the discrete sampling ($N = 10^5$ particles) of the phase probability distribution as a function of $\theta = \mathrm{mod}(q_c x, 2\pi) - \pi$ in both a linear (bottom right) and polar (top right) plot. In the bottom right panel of Figs. b-d, the black dashed line indicates the uniform probability value $\frac{1}{2\pi}$. Parameters are: $\delta = +15\Gamma$, $T = 300\,\mu$K, $b_0 = 100$, $d = 5$ mm and $R = 1$. The injected pump is $p_0 = 0.043$ (5% above threshold). A movie displaying the dynamics of the system for a pump duration of 5 ms has also been submitted as electronic supplementary material.

We numerically solved the coupled dynamics (3.1-3.2) of the phase-space distribution $f(x, v, t)$ and the optical field in one transverse dimension using a semi-Lagrangian method with spline interpolation [15]. The initial condition of the gas is set to be a Lorentzian distribution with full-width-at-half-maximum v_{th}: $f_0(v) = v_{\mathrm{th}}/[\pi(v^2 + v_{\mathrm{th}}^2)]$. Our numerical results confirm the theoretical predictions reported in the previous Sections since above threshold a spatially homogeneous cloud is spontaneously converted into a periodic pattern with periodicity $\Lambda_c = 2\pi/q_c$. Driving the system 5% above threshold, we monitor the bunching parameter r and observe a transition from a $r = 0$ state to a state characterised by $r > 0$, followed by oscillations with a period of about $T_{\mathrm{slosh}} \simeq 800\,\mu$s, see Fig. 4a. This is analogous to what is observed in inviscid CARL [29], and is due to the atoms sloshing and periodically amplifying in the spontaneously formed optical potential. Fig. 4b, 4c and 4d show the formation of complementary periodic spatial structures for the optical intensity $s(x)$ and the atomic density $n(x)$. The spatial scale of the pattern is $\Lambda_c \simeq 120\,\mu$m for our choice of parameters, and is in good agreement with the experimental observations [16]. The depth of the modulated potential shown in Fig. 4d in units of temperature is $T_{\mathrm{pot}} \approx \frac{\hbar\delta(s_{\max} - s_{\min})}{k_B} \approx 440\mu$K, where $s_{\max}$ and $s_{\min}$ are the maximum and

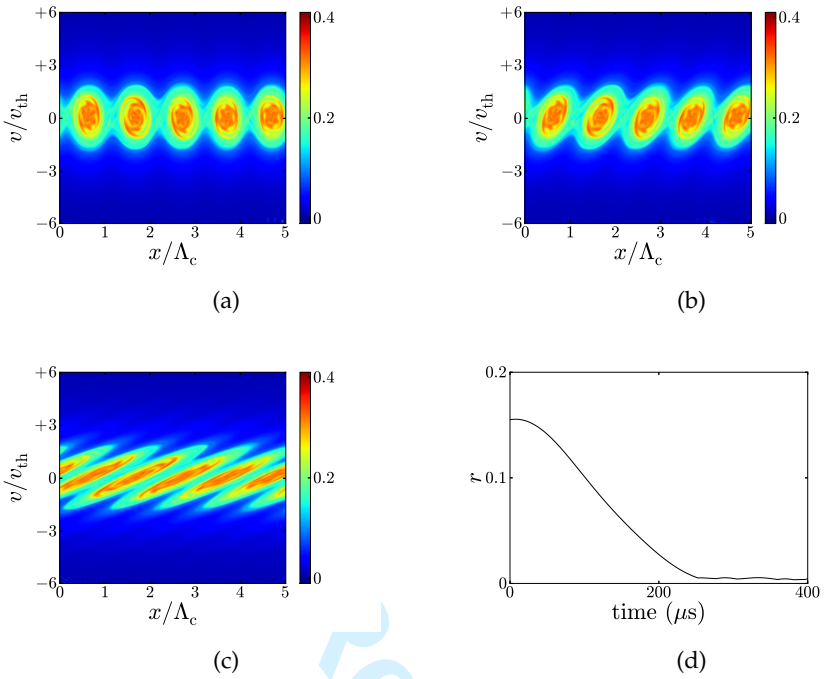

Figure 5: Numerical results for the dephasing dynamics. The upper left panel (a) shows the distribution function for a pump duration of 5 ms, obtained for the same parameters as Fig. 4. The pump is subsequently switched off and the atomic cloud state is monitored after 100 μs (b) and 500 ms (c). The bunching factor decreases monotonically with a characteristic dephasing time of the order of 100 μs (d).

minimum values of s respectively and k_B is the Boltzmann constant. For each of these states we calculate the probability distribution of the phase θ by sampling the density distribution $n(\theta)$ with $N = 10^5$ particles, which shows a peak around the value $\psi \simeq \pi/2$ in correspondence with the synchronisation transition.

Fig. 5 shows the dynamics of the pattern obtained for the same parameters as Fig. 4 when the injected pump is switched off after 5 ms. As the system is left with no driving ($K = 0$), the ballistic motion of the atoms leads to a dephasing dynamics in which the bunching factor r decreases monotonically, see Fig. 5d. The phase space distribution $f(x, v)$ is monitored just before switching off the pump (Fig. 5a), and then after 100 μs (Fig. 5b) and 500 μs (Fig. 5c). The characteristic dephasing time can be inferred from Fig. 5d, and is in the order of 100 μs. This is consistent with the timescale of atomic motion at the considered temperature, and agrees with our experimental results, see Fig. 3.

5. Conclusion

Self-structuring of the atomic density in a cloud of a cold atomic gas that is optically pumped can be interpreted as a transition to a synchronised state of Kuramoto oscillators. Although this connection was made in cases where strong damping is present [7,20], we have shown that the analogy can be extended to cases where no damping is present such as those of the experimental realisation in [16]. In this case a finite spread exists in the natural frequency distribution of the fictitious oscillators, which sets the threshold for the synchronisation transition.

We note that a similar coupling between the optical field and the motion of atoms can also arise

in the context of cooperative scattering of light by an optically thick cloud of atoms [30]. It is possible to derive the optical forces acting on each atom in an ensemble of N atoms including both the quasi-resonant radiation pressure (dominant close to the atomic resonance) as well as the optical dipole forces (more relevant for larger detuning) [31]. In contrast to the situation considered in this article, in [30,31] these forces arise from direct dipole-dipole coupling between atoms and are not mediated via a propagation and feedback through a mirror. Furthermore, we expect that synchronisation between different atoms not only manifests itself in the motional degrees of freedom, but can also affect the internal degrees of freedom of the atoms, leading to synchronised cooperative scattering of a large cloud. Such cooperative scattering has been investigated in pioneering work by R. Dicke for samples smaller than the wavelength but also for 'radiation of gas of large extent' [31].

Finally, it is important to mention that our theoretical and numerical predictions of the Kuramoto analogy for inviscid systems can be applied outside the interaction of light with cold atoms. For example it is possible to connect cold atoms and plasmas via the correspondence between dipole and ponderomotive forces. Attractive (shadow) and repulsive (radiation pressure) forces exist inside magneto-optically trapped samples, which introduce an effective charge between the atoms and thus simulate electrostatic interactions. Self-structuring and its Kuramoto interpretation are then to be expected in the investigation of various plasma systems without friction, possibly including quantum plasmas.

In the context of the special issue, it is important to mention that optomechanical solitons were predicted in single-pass propagation [13] and cavity schemes [12] with velocity damping. Corresponding structures are expected for the single-mirror geometry.

Acknowledgment

Financial support from the Leverhulme Trust (research grant F/00273/0) and the Engineering and Physical Sciences Research Council (for GRMR - grant EP/H049339) is gratefully acknowledged. We are grateful to R. Martin for computational support. The collaboration between the two groups was supported by the Royal Society (London).

References

1. H. Ritsch, P. Domokos, F. Brenneke and T. Esslinger 2013 Cold atoms in cavity-generated dynamical optical potentials, *Rev. Mod. Phys.* **85**, 553-601
2. P. Domokos and H. Ritsch 2002 Collective cooling and self-organization of atoms in a cavity, *Phys. Rev. Lett.* **89**, 253003
3. A.T. Black, H.W. Chan and V. Vuletić 2003 Observation of collective friction forces due to spatial self-organization of atoms: from Rayleigh to Bragg scattering, *Phys. Rev. Lett.* **91**, 203001
4. K. Baumann, C. Guerlin, F. Brennecke and T. Esslinger 2010 Dicke quantum phase transition with a superfluid gas in an optical cavity, *Nature* **464**, 1301-1306
5. R. Bonifacio and L. de Salvo 1994 Collective atomic recoil laser (CARL) optical gain without inversion by collective atomic recoil and self-bunching of two-level atoms, *Nucl. Instrum. Methods Phys. Res. A* **341** 360-362
6. D. Kruse, C. von Cube, C. Zimmermann and Ph.W. Courteille 2001 Observation of lasing mediated by collective atomic recoil, *Phys. Rev. Lett.* **91**, 183601
7. C. von Cube, S. Slama, D. Kruse, C. Zimmermann, Ph.W. Courteille, G.R.M. Robb, N. Piovella and R. Bonifacio 2004 Self-synchronization and dissipation-induced threshold in collective atomic recoil lasing, *Phys. Rev. Lett.* **93**, 083601
8. J.A. Greenberg and D.J. Gauthier 2012 High-order optical nonlinearity at low light levels, *Eur. Phys. Lett.* **98**, 24001
9. J.A. Greenberg and D.J. Gauthier 2012 Steady-state, cavityless, multimode superradiance in a cold vapor, *Phys. Rev. A* **86** 013823
10. J.A. Greenberg, B.L. Schmittberger and D.J. Gauthier 2011 Bunching-induced optical nonlinearity and instability in cold atoms, *Opt. Expr.* **19**, 22535-22549

11. E. Tesio, G.R.M. Robb, T. Ackemann, W.J. Firth and G.-L. Oppo 2012 Spontaneous optomechanical pattern formation in cold atoms, *Phys. Rev. A* **86**, 031801(R)
12. E. Tesio, G.R.M. Robb, T. Ackemann, W.J. Firth and G.-L. Oppo 2013 Dissipative solitons in the coupled dynamics of light and cold atoms, *Opt. Expr.* **21**, 26144-26149
13. M. Saffman and Y. Wang 2008 Collective focusing and modulational instability of light and cold atoms in *Dissipative solitons: from optics to biology and medicine*, *Lect. Notes Phys.* **751**, 361
14. M.A. Muradyan, Y. Wang, W. Williams and M. Saffman 2005 Absolute instability and pattern formation in cold atomic vapors in *Trends in Optics and Photonics (TOPS)*, vol. **80**, Nonlinear Applications, OSA Technical Digest (OSA, Washington, D.C., 2005), paper ThB29
15. E. Tesio, G.R.M. Robb, T. Ackemann, W.J. Firth and G.-L. Oppo 2014 Kinetic theory for transverse optomechanical instabilities, *Phys. Rev. Lett.* **112**, 043901
16. G. Labeyrie, E. Tesio, P. M. Gomes, G.-L. Oppo, W.J. Firth, G.R.M. Robb, A.S. Arnold, R. Kaiser and T. Ackemann 2014 Optomechanical self-structuring in cold atomic gases, *Nat. Phot.* **8**, 321-325
17. S. Gopalakrishnan, B.L. Lev and P.M. Goldbart 2011 Frustration and glassiness in spin models with cavity-mediated interactions, *Phys. Rev. Lett.* **107**, 277201; P. Strack and S. Sachdev 2011 Dicke Quantum Spin Glass of Atoms and Photons, *Phys. Rev. Lett.* **107**, 277202
18. S.H. Strogatz 2003 *Sync: The emerging science of spontaneous order*, Hyperion
19. S. Gupta, M. Potters and S. Ruffo 2012 One-dimensional lattice of oscillators coupled through power-law interactions: continuum limit and dynamics of spatial Fourier modes, *Phys. Rev. E* **85**, 066201
20. J. Javaloyes, M. Perrin and A. Politi 2008 Collective atomic recoil lasing as a synchronization transition, *Phys. Rev. E* **78**, 011108
21. J. A. Acebròn, L.L. Bonilla and C.J. Pérez Vicente, F. Ritort and R. Spigler 2005 The Kuramoto model: a simple paradigm for synchronization phenomena, *Rev. Mod. Phys.* **77**, 137-185
22. W.J. Firth 1990 Spatial instabilities in a Kerr medium with single feedback mirror *J. Mod. Opt.* **37**, 151-153; G. D'Alessandro and W.J. Firth 1991 Spontaneous hexagon formation in a nonlinear optical medium with feedback mirror, *Phys. Rev. Lett.* **66**, 2597-2600
23. W.H.F. Talbot 1836 Facts relating to optical science. No. IV, *Philos. Mag.* **9**, 401-407
24. E. Ciaramella, M. Tamburrini and E. Santamato 1993 Talbot assisted hexagonal beam patterning in a thin liquid crystal film with a single feedback mirror at negative distance, *Appl. Phys. Lett.* **63**, 1604-1606
25. T. Ackemann and W. Lange 2001 Optical pattern formation in alkali metal vapors: mechanisms, phenomena and use, *Appl. Phys. B* **72**, 21-34
26. P.W. Smith, A. Ashkin and W. Tomlinson 1981 Four-wave mixing in an artificial Kerr medium, *Opt. Lett.* **6**, 284-286
27. P.J. Reece, E.M. Wright and K. Dholakia 2007 Experimental observation of modulation instability and optical spatial soliton arrays in soft condensed matter, *Phys. Rev. Lett.* **98**, 203902
28. W. Man, S. Fardad, Z. Zhang, J. Prakash, M. Lau, P. Zhang, M. Heinrich, D.N. Christodoulides and Z. Chen 2013 Optical nonlinearities and enhanced light transmission in soft-matter systems with tunable polarizabilities, *Phys. Rev. Lett.* **111**, 218302
29. T. Grießer, H. Ritsch, M. Hemmerling and G.R.M. Robb 2010 A Vlasov approach to bunching and selfordering of particles in optical resonators, *Eur. Phys. J. D* **58**, 349-368
30. T. Bienaime, S. Bux, E. Lucioni, Ph.W. Courteille, N. Piovella and R. Kaiser 2010 Observation of cooperative radiation pressure in presence of disorder, *Phys. Rev. Lett.* **104**,183602
31. Ph.W. Courteille, S. Bux, E. Lucioni, K. Lauber, T. Bienaime, R. Kaiser and N. Piovella 2010 Modification of radiation pressure due to cooperative scattering of light, *Eur. Phys. J. D* **58**, 69
32. R.H. Dicke 1954 Coherence in spontaneous radiation processes, *Phys. Rev.* **93**, 99